ABSTRACT

PRESSLEY, PHILLIP NATHANIEL. Fuel Production from Municipal Solid Waste: A Life-Cycle Assessment. (Under the direction of Dr. Tarek N. Aziz and Dr. Joseph F. DeCarolis).

As energy prices have increased, interest in alternative energy production methods has grown. Municipal solid waste (MSW) is a promising alternative energy source because of its abundance and low cost. Landfill gas-to-energy and waste-to-energy, the most common MSW energy recovery processes, produce electricity. However, an MSW-derived feedstock can be treated via gasification and Fischer-Tropsch (FT) processes to create diesel, gasoline, and other refined products. Though such fuel production is technically feasible, no research has explored the environmental impacts of the creation and combustion of fuel from MSW. To fill a gap in the existing literature, a life-cycle assessment (LCA) was conducted to quantify the global warming potential, energy consumption, and energy production of a converting MSW to liquid fuels via a gasification/FT process.

The modeled process begins with the mechanical separation of collected MSW. MSW components with high moisture content (i.e., food waste), high pollution potential (i.e., PVC), and low energy content (i.e., glass, metals) are removed. The remaining stream, which is converted into a refuse-derived fuel (RDF), is composed primarily of paper and plastic. RDF is then fed to a gasifier where it is transformed into syngas, which consists primarily of CO, H_2, CO_2, and CH_4. Upon exiting the gasifier, syngas is purified and pressurized. Pressurized syngas is converted to synthetic crude oil (syncrude) via FT and a gaseous hydrocarbon blend. Syncrude is refined into a set of products that include transportation fuels.

This LCA begins when collected MSW is delivered to the RDF facility and includes emissions associated with RDF production, gasification, FT, refinement, FT fuel combustion, and inter-facility transportation. At all stages, both direct (i.e., onsite fuel use) and indirect emissions (i.e., emissions from offsite electricity generation) are aggregated. FT fuel combustion is included because CO_2-biogenic, which is produced by the combustion of biogenic MSW components, does not contribute to GWP. The functional unit for this study is one megagram (Mg) of MSW delivered to the RDF facility.

This study found that 110 L of gasoline and 51 L of diesel are produced along with 70 kg of other FT products and 180 kWh of electricity for every Mg delivered to the RDF facility. The process consumes 4.6 GJ of energy while creating fuels with a cumulative energy content of 9.7 GJ. However, the net global warming potential is -112 kg of CO_2-e. Sensitivity analysis revealed that decreasing fossil content in MSW decreased GWP and fuel production simultaneously. Technological advancement resulting in higher CO reaction rates or lower pressure requirements in the FT reactor will result in significant decrease in GWP. The modeled system is also sensitive to exogenous changes to the electricity grid mix. For example, as CO_2-fossil emissions decrease for every kilowatt-hour of electricity produced by the grid, the net GWP of the modeled system also decreases.

Fuel Production from Municipal Solid Waste: A Life-Cycle Assessment

by
Phillip Nathaniel Pressley

A thesis submitted to the Graduate Faculty of
North Carolina State University
in partial fulfillment of the
requirements for the degree of
Master of Science

Environmental Engineering

Raleigh, North Carolina

2013

APPROVED BY:

_____	_____
Tarek N. Aziz Committee Co-Chair	Joseph F. DeCarolis Committee Co-Chair

_____
Morton A. Barlaz

BIOGRAPHY

Phillip Pressley was born a Wolfpack fan in western North Carolina. Upon graduation from high school, he attended North Carolina State University. Here he watched all-kinds of Wolfpack sports, regardless of their performance on the field. In 2011, Phillip completed the University Honors Program and graduated summa cum laude from North Carolina State University with a Bachelor of Science in Civil Engineering. He remained at North Carolina State to pursue a Master of Science in Environmental Engineering. On October 31, 2012, Phillip officially retired from intramural soccer after scoring his first career goal. Phillip finished both the coursework and research for his first graduate degree in Spring 2013.

TABLE OF CONTENTS

LIST OF TABLES

LIST OF FIGURES

CHAPTER 1

1. Introduction

Interest in clean, affordable energy and diversion of waste from landfills drives interest in energy recovery from municipal solid waste (MSW). As an energy feedstock, MSW is abundant and delivered to treatment facilities at negative cost, i.e., waste producers pay tipping fees for the disposal of the 260 million tons produced annually in the US (US EPA, 2010). Many energy recovery options from solid waste exist, including landfill gas-to-energy, incineration, anaerobic digestion, and gasification. Life cycle assessment (LCA) can be employed to evaluate the relative energy and environmental performance of such options from curb to ultimate disposal, yielding insights that inform public policy and investment decisions (e.g., Kaplan et al., 2009; Levis and Barlaz, 2011).

LCA has previously been used to characterize the environmental performance of energy recovery options from MSW by accounting for all process-related energy and emissions, both direct and indirect. For example, landfill gas-to-energy studies include emissions associated with curbside collection processes, fugitive methane, electricity generation, and heavy machine operation (Menard et al.,2004; Kaplan et al., 2009; Levis et al., 2011). Waste-to-energy studies account for emissions associated with curbside collection processes, energy use, electricity generation, and ash management (Harrison et al., 2000; Riber et al., 2008; Koehler et al., 2011). Other options for energy recovery from solid waste exist, including conventional gasification, torrefaction, pyrolysis, and plasma arc gasification, but scarce operational data has prevented the evaluation of their life cycle impacts .

This paper describes an LCA that evaluates the conversion of an MSW-derived feedstock into a liquid hydrocarbon, similar to crude oil, via gasification and Fischer-Tropsch (FT). A unique feature of the gasification-FT pathway – relative to many other MSW energy recovery options which ultimately produce electricity – is that it produces a set of high value liquid transportation fuels. Gasification thermo-chemically converts a solid feedstock into a synthesis gas (i.e., syngas), which is primarily comprised of carbon monoxide, diatomic hydrogen, and carbon dioxide (Lee et al., 2007). Syngas is then passed over an iron- or cobalt-based catalyst in a FT reactor (Spath and Dayton, 2003). The resultant synthetic crude oil (i.e., syncrude) represents a valuable energy commodity that can be processed in an existing petroleum refinery into liquid transportation fuels. Several commercial and governmental entities have pursued commercial MSW gasification over the last decade (Pytlar, 2010), and full-scale FT technology is currently used to create liquid transportation fuels (Cao et al., 2008). The gasification of several MSW components has been demonstrated experimentally (Ahmed, 2009; Gai, 2012), but it has never been combined with FT technology in a commercial application.

Though gasification and FT demonstrations have been limited, many computer-based models simulate the chemical reactions within gasifiers and FT reactors. Thermodynamic equilibrium models can predict syngas yield and composition from gasifiers (Vera et al., 2013; Shabbar and Janajreh, 2011; Sreejith et al., 2011); however, many require process expertise and utilize complex proprietary software, such as ASPEN Plus[1] or Cycle-Tempo[2].

[1] More information about ASPEN Plus can be found at http://www.aspentech.com/products/aspen-plus.aspx
[2] More information about Cycle-Tempo can be found at http://www.cycle-tempo.nl/

LCA requires simpler, reduced-form models to estimate the yield of FT fuels and other products that are responsive to changes in the input waste composition. Models have been developed to estimate syngas yield (Fock et al., 2000) and FT product distribution (Flory, 1936), but no existing reduced-form models predict both syngas composition and FT fuel yield for LCA use.

While LCA has also been used to evaluate the environmental performance of biomass gasification processes (Carpentieri et al.,2005) and biomass conversion to transportation fuel technologies, including FT (Swain et al.,2011), it has not been applied to the gasification and conversion of solid waste to transportation fuels. RTI (2012) conducted an LCA that estimated environmental impacts associated with fuel production from MSW; however, they did not include the processing required to convert MSW into a suitable gasifier feedstock (RTI International, 2012).

This paper fills a gap in the literature by quantifying the energy use and greenhouse gas emissions associated with the conversion of MSW to refined fuel products via gasification and FT. To conduct this LCA, we developed a simplified spreadsheet model that aggregates the process-related emissions from waste separation through fuel combustion. A key challenge was the development of a reduced-form model appropriate for LCA that predicts the syngas and syncrude compositions based on calibration to complex chemical equilibrium models associated with gasification and FT. The model results include mass flows between each process within the system boundary and the associated energy production, energy consumption, and global warming potential (GWP). Model sensitivity to MSW composition and key model input parameters is also explored.

2. Methodology

2.1 LCA System and Process Description

The functional unit in this LCA is 1 megagram (i.e., 1 metric ton) of mixed waste delivered to a sorting facility that produces a refuse-derived fuel (RDF) suitable for a gasifier. As a result, the system boundary for the proposed MSW to liquid fuels system includes mechanical MSW processing, gasification, FT, transportation, and refined product combustion as shown in Figure 1. MSW is mechanically processed into RDF to increase the calorific value and reduce the moisture content. RDF is fed into a gasifier where thermochemical processing transforms RDF into a mixture of carbon monoxide (CO), diatomic hydrogen (H_2), carbon dioxide (CO_2), and methane (CH_4) called syngas (Lee et al.,2007). Syngas is pressurized and purified to remove contaminants harmful to downstream processes, and then run through FT reactors, where CO and H_2 are converted into longer chain liquid hydrocarbons (Spath and Dayton, 2003). The liquid portion forms syncrude, a mixture of hydrocarbons similar to crude oil. Syncrude is transported from the FT facility to an oil refinery, which produces gasoline, diesel, and other refined products. The GWP of biogenic CO_2 was considered to be zero. As such, the combustion of refined products derived from syncrude is considered within the system boundary to capture the effects of its lower GWP. Offsets associated with liquid fuel production from MSW are estimated by subtracting the GWP associated with the production and combustion of an equivalent mass of petroleum-derived fuel.

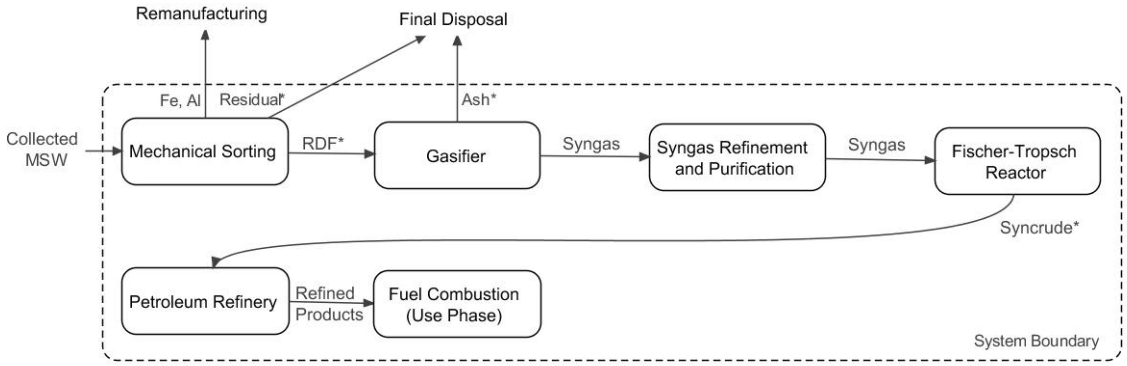

Figure 1 High-Level Mass Flow Diagram. MSW is mechanically sorted to create RDF, which is treated via gasification and the FT processes to produce liquid fuels. Fuel combustion is included within the system boundary to capture the GWP benefits associated with the biogenic fraction of RDF. Transportation is included for materials followed by (*).

The MSW to liquid fuel LCA spreadsheet model developed for this analysis uses a process-based LCA approach to aggregate the consumption and production of energy and greenhouse gas emissions associated with each process in Figure 1. The model does not account for emissions associated with the curbside collection of MSW, since curbside collection must take place in any case. The final system emissions account for energy use, energy offsets, and fuel combustion. The impacts of interest are total energy consumption and GWP. Other impact categories are not examined because comprehensive empirical data are not available for syngas contaminants and residual/effluent from pollution control devices.

The model uses life-cycle inventory (LCI) data from the National Renewable Energy Laboratory's US Life-Cycle Inventory (NREL LCI) Database (2012) to estimate the product yields and emissions resulting from syncrude refinement. Combustion data for produced and

offset fuels was taken from EcoInvent (2010). Inter-facility transportation emissions are included, since the RDF facility, gasifier/FT units, and refinery are unlikely to be co-located. The modeled transportation modes and corresponding distances, provided in Table A1, were chosen to reflect a case representative of the U.S. east coast in which all waste disposal occurs in Raleigh, NC, but transportation to the refinery requires truck transport to a coastal port in Wilmington, NC and shipping via tanker to Galveston, TX.

2.2 Gasification Feedstock Production from MSW

The transformation of MSW to a liquid transportation fuel begins with the delivery of collected MSW to an RDF production facility, as shown in Figure 1. MSW processing is included in this analysis because gasification process studies note the benefits of shredding and pelletization of MSW-derived feedstocks on product yield (Ruoppolo et al.,2012; Ammendola et al.,2012) , but such processing requires energy use and produces environmental impacts. To prepare MSW for gasification, the RDF facility removes materials with low-calorific values (e.g., metals, glass), high moisture content (e.g., food waste, yard waste), and process-harmful combustion emissions (e.g., polyvinyl chloride) from the input MSW stream. The remaining waste stream, consisting primarily of paper and plastic, is shredded and pelletized to form RDF that is transported to the gasification facility via heavy-duty truck. A detailed process flow diagram and discussion of the RDF facility is presented in Appendix B.

The model of RDF production uses MSW composition, equipment energy consumption, and equipment-specific separation efficiencies to calculate the mass of each waste fraction removed by each piece of equipment based on updates to Combs (2012).

These calculated mass flows are combined with equipment-specific throughput capacity factors and energy data to estimate total facility energy consumption. Throughput-based equipment sizing implicitly assumes a linear relationship between throughput and equipment energy consumption, thereby preventing inappropriately-sized equipment from biasing results. In an effort to model a gasifier with high syngas yield, the high-level process shown in Figure 2 was developed to maximize the calorific value of RDF while removing undesirable materials.

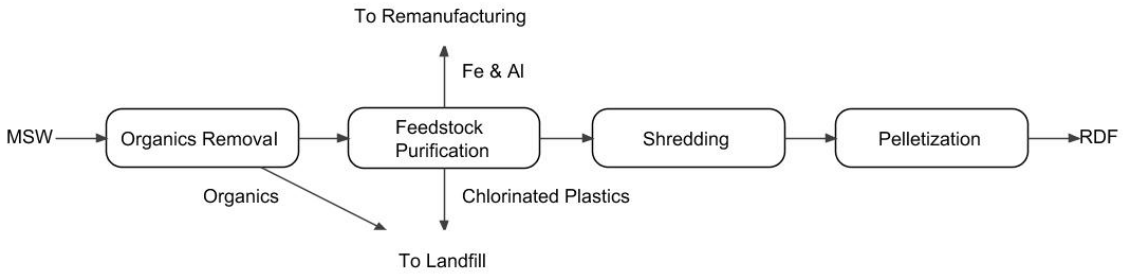

Figure 2 Conceptual diagram of RDF processing. RDF is created by mechanically removing wet organics (e.g., food and yard waste), metals, and chlorinated plastics, before shredding and pelletizing the remaining material, composed primarily of paper and plastic. A more detailed, process-specific mass flow diagram is provided in Figure B1 in Appendix B.

2.3 Gasification

The estimated RDF composition and gasifier input parameters are used to calculate syngas composition in the gasification module. The gasifier inputs include the gasifier performance parameters and feedstock material properties shown in Table 1.

Table 1 Required Gasifier Input Parameters

Feedstock Material Properties	Gasifier Performance Parameters
Biogenic Carbon Content Fossil Carbon Content Hydrogen Content Oxygen Content Lower Heating Value Ash Content Moisture Content Total Volatile Solids	Air requirement per megagram of feedstock H_2 to CO ratio CH_4 (as % of Total Solids) Total Volatile Solids Unreacted (%)

The air requirement and H_2 to CO ratio for all feedstock components in this analysis were based on ASPEN Plus simulations of a fluidized bed gasifier operating at 900^{o}C and 1 atmosphere. The key settings and assumptions for the ASPEN Plus simulation model are given in Table 2. For each homogeneous feedstock listed in Table C1, material properties are combined with a 500 Mg per day throughput to estimate syngas yield. The feedstocks were treated as non-conventional components in the ASPEN simulation with heating values from ECN (2012). ASPEN Plus RYield and RGibbs blocks were used to simulate RDF gasification. In the RYield block, the feedstock is decomposed into its constituent elements (e.g., C, H, O) and inert ash based on the ultimate analysis. The decomposed elements are combined with air and introduced into the RGibbs reactor. The parameters listed in Table 2 were used as constraints. Thermodynamic equilibrium uses the principle of Gibbs free energy minimization and atomic species balances to determine all possible product combinations from the RGibbs block. We derived the H_2 to CO ratio and air requirement for each RDF component from the simulations for use in the gasifier spreadsheet model. To estimate compression requirements, a 4 stage compressor with an intercooler pressurized

syngas to 20 atm. The net heat duty of the gasifier is equal to the sum of the heat input and output of the RYield and RGibbs blocks and the gasifier heat loss, which was assumed to be 1 % of the total thermal input.

Table 2 Key assumptions used in the ASPEN Plus simulations of the gasifier

Ambient condition	T=25 °C, P=1 atm
Air	79% N_2, 21% O_2 by volume
Reaction assumptions	all reactions reach thermodynamic equilibrium
Reactors Models	RYield, RGibbs
Property method	PR-BM
Stream class	MIXCINC
Databank	COMBUST, INORGANIC, SOLIDS, PURE
Heat loss in the CDCL system	1% of the total thermal input
Compressor specifications	4 stage with intercooler at 40°C Isentropic efficiency is 0.8 Mechanical efficiency is 1

The gasifier input parameters are used with mass balance equations to estimate syngas yield and composition. The fundamental system mass balance for every waste component *i*, displayed in Equation 1, shows all mass flowing into the system on the left and all mass leaving the system on the right.

$$m_{air,i} + m_{s,i} + m_i = m_{CO,i} + m_{H_2,i} + m_{CO_2,i} + m_{CH_4,i} + m_{ash,i} + m_{H_2O,i}$$ (Equation 1)

where:

$m_{air,i}$ mass of air input to gasifier that reacts with waste fraction *i*

$m_{S,i}$ mass of steam that reacts with waste fraction *i*

m_i mass of waste fraction *i* input to gasifier.

$m_{CO,i}$ mass of CO resulting from gasification of m_i

$m_{H2,i}$ mass of H_2 resulting from gasification of m_i

$m_{CO2,i}$ mass of CO_2 resulting from gasification of m_i

$m_{CH4,i}$ mass of CH_4 resulting from gasification of m_i

$m_{ash,i}$ mass of ash resulting from gasification of m_i

$m_{H2O,i}$ mass of water resulting from gasification of m_i; unreacted excess steam that exits the gasifier

Syngas yield and composition are calculated independently for each waste component within the RDF. Each waste component has a specified H_2 to CO ratio, and the yield of H_2 and CO varies by component. The total syngas yield is the summation of each feedstock component's syngas yield. Interactivity between heterogeneous RDF components is not considered because no known analytical method can estimate syngas yield from the interaction of heterogeneous materials (Ahmed et al.,2011), and no empirical data about the interaction of all waste components is available. If the H_2 to CO ratio associated with the total syngas yield is lower than the ratio required for effective processing in a FT reactor, the model accounts for the addition of steam to enable the water-gas shift reaction (Marano and Ciferno, 2001). As shown in Equation 2, steam interacts with CO to form H_2 and CO_2 in the water-gas shift reaction. The resulting CO_2 is allocated to waste fractions by multiplying the total CO_2 produced through water-gas shift by the fraction of total CO created by the waste fraction. Thus, the CO transformed by water-gas shift from each waste fraction is proportional to the waste fraction's contribution to total CO.

$$CO + H_2O \rightarrow CO_2 + H_2$$ (Equation 2)

This mass balance approach simplifies the estimation of syngas composition and yield and neglects feedstock component interactivity, which represents a simplifying assumption that must be made in the absence of more experimental data.

The results from the spreadsheet model were compared with results from the ASPEN Plus simulations used to generate the H_2 to CO ratio and air requirement for each RDF component. Assuming 0% CH_4 production from each feedstock, the spreadsheet model estimated the CO and H_2 yields within 10% of ASPEN Plus for all feedstocks with moisture contents less than 10%, as shown in Appendix C, Tables C1 and C2. In this analysis, we used 3% CH_4 for all biogenic components (Southern Research Institute, Personal Communication). The plastic components were modeled with 0% CH_4 because the ASPEN Plus simulations revealed CH_4 production was negligible (<0.25% of CO molar production).

2.4 Syngas Purification

Syngas exiting a gasifier contains impurities from the feedstock. The composition and quantity of the impurities in syngas from an MSW-fed gasifier are largely unknown, making purification technology selection uncertain (Belgiorno, 2003) and preventing accurate estimation of non-energy inputs and wastes. In previous work, energy consumption of conventional WTE facility components, including incinerator management technology and air pollution control equipment, was modeled as house load, a single parameter representing facility electricity demand (Harrison et al.,2000). Similarly in this analysis, a portion of the gasification facility's energy requirements are modeled as a house load, such that the electricity requirements of gasification monitoring equipment and syngas purification technology are denoted as a percentage of the feedstock energy content on an LHV basis.

The house load does not include energy associated with the compressor used to give the syngas a CO partial pressure of 20 bar, which was included separately. The compressor was removed from the house load because the energy consumption calculated using ASPEN Plus was 500 kWh per Mg of gasified feedstock, which was a significant fraction of the total energy consumption used to process the feedstock. Sensitivity of model results to compressor energy use and the house load is discussed in Section 3.6.

2.5 Fischer-Tropsch and Refinement

FT product yields are estimated using the Anderson-Schulz-Flory (ASF) distribution equation, shown in Equation 3 (Spath and Dayton, 2003), along with the assumed CO conversion efficiency and syngas composition. The ASF equation estimates the weight distribution of carbon chain lengths. In this analysis, a chain growth probability, or α-value, of 0.95 is used to describe the FT reaction that produces syncrude with a hydrocarbon distribution similar to crude oil (Claeys and van Steen, 2004). The modeled system includes two FT reactors in series to increase the CO conversion rate. The catalyst reacts 60% of the input CO in each reactor, so two reactors have a total reaction of 84% of initial CO (i.e., 60% in the first reactor and 60% of the unreacted 40% in the second reactor). The ASF carbon chain length weight fractions are then summed over the relevant carbon chain ranges shown in Table 3 to produce product weight fractions, which are combined with input mass (calculated from syngas composition) to estimate the unrefined product yield. Modeling the unrefined product yield allows for variation in onsite treatment and transportation requirements, creating the flexibility to examine multiple refinery scenarios. The total syncrude yield is calculated using the total reformed syngas mass. Syncrude yield is

allocated to individual waste fractions based on their contribution to total CO, similar to the CO_2 produced as a result of the water-gas shift reaction.

$$W_n = n \cdot (1-\alpha)^2 \alpha^{n-1} \qquad \text{(Equation 3)}$$

where:
W_n weight fraction for carbon chain length n
α chain growth probability
n carbon chain length

Table 3 Carbon Chain Length Ranges for Unrefined FT Products (Based on Spath and Dayton, 2003)

Hydrocarbon Type	**Carbon-Length Range**
Gaseous	1 – 4
Light Liquid	5 – 11
Diesel	12 – 20
Heavy Liquid	21 – 25
Solids	26 +

For simplicity, gaseous hydrocarbons are assumed to be removed from the unrefined FT products. The gas is used to fuel a combustion turbine that generates electricity at 40% efficiency. In addition, heat is recovered during syngas cooling and from the exothermic FT reaction. The heat available from syngas cooling was estimated using ASPEN Plus, and the heat created from the FT reaction was calculated using reaction chemistry (Spath and Dayton, 2003). In this analysis, we assume that 30% of this generated heat can be converted into electricity, which offsets grid electricity. Though the model has the functionality to include further distillation onsite, it is assumed that all liquid hydrocarbons are transported to

an existing petroleum refinery located offsite. RDF mass flow from a single facility produces a low volume of FT products compared to the throughput of a conventional petroleum refinery. Thus, construction of a full-scale refinery with its many energy intensive unit processes (e.g., distillation, hydrotreating) was not considered a cost-effective alternative (Pellegrino et. al.,2007).

The NREL LCI database (2012) includes a petroleum refining entry with refinery outputs. Our model equates a kilogram of liquid FT products (syncrude) with a kilogram of crude oil. Thus, FT and petroleum production are modeled with identical product distributions and fuel combustion emissions. Because FT products are low in sulfur and other impurities, refineries may bypass some purification processes, reducing the syncrude refinement energy consumption (Marano and Ciferno, 2001). Due to the small contribution of syncrude to the total refinery throughput; however, in the present analysis syncrude and fossil-based crude oil are assumed to undergo the same amount of refinement. Syncrude is transported 250 kilometers via truck to a coastal port followed by 2700 kilometers of ocean freighter transport to a refinery. The refinery produces diesel, gasoline, liquefied petroleum gas (LPG), kerosene, residual fuel oil, refinery gas, bitumen, and petroleum coke from syncrude (NREL, 2012).

Refined products from both crude and syncrude are distributed together and assumed to have equal energy densities. However, there may be substantial differences in the GWP associated with the combustion of MSW derived FT products, depending on the biogenic fraction of waste in MSW.

3. Model Results

To quantify the energy and environmental performance of converting MSW to liquid fuels, we examined the mass flow, fuel yields, energy consumption, and GWP based on an assumed input waste composition. From an LCA perspective, the mass flow and process yields represent intermediate results rather than impacts, but they enable comparison with other gasification feedstocks and fuel-producing processes.

3.1 Mass Flow

The RDF facility separates the delivered MSW, with US national average composition derived from US EPA (2010) and shown in Table A2, into RDF, recyclable ferrous and aluminum, and a residual stream that is transported to the location of final disposal (e.g., landfill). Of the collected MSW mass, 56 % is recovered as RDF and 2% as recyclable metals, with the remaining 42% being residual. As shown in Table 4, each material entering the RDF facility constitutes a different share of each RDF facility output. Recyclable paper and plastic make up 56% of the RDF. If single-stream recycling is implemented in a system with gasification, significant changes in RDF composition should be expected.

Table 4 Composition of RDF Facility Output Streams. The RDF facility separates the national average input waste composition, derived from US EPA (2010) and located in Table A2, into three streams with three different compositions.

	Composition of:		
	RDF	**Recycled Metals**	**Residuals**
Recyclable Fiber	47%	0%	0%
Recyclable Plastic	8%	0%	0%
Non-Recyclable Fiber	20%	0%	0%
Non-Recyclable Plastic	11%	0%	0%
Ferrous	0%	58%	0%
Aluminum	0%	42%	0%
Other Organics	14%	0%	78%
Other Inorganics	0%	0%	22%

3.2 Gasification

Using the calculated RDF composition, syngas yield is estimated per unit mass, as shown in Table 5. The mass of CH_4 produced in the gasifier is 3% of the total solids of biogenic carbon input and 0% of the total solids of fossil carbon (i.e., plastics) input. Because 19 % of RDF is of fossil origin, only 1.9 kilomoles (84 kg) of produced CO_2 and 0.2 kilomoles (3.0 kg) of produced CH_4 contribute to GWP.

Table 5 Syngas Composition and Yield. The calculated RDF composition is used to estimate syngas yield and composition

	CO	H_2	CO_2	CH_4
Yield (10^3 moles/ Mg MSW)[A]	7.4	14.8	10.1	1.0

[A] To convert the values in Table 5 to units of yield per mass of RDF, divide the values by 0.56, the fraction of MSW that becomes RDF.

3.3 FT Yields

The calculated syngas yield was used with the ASF equation to estimate syncrude yield from the two FT reactors. The 16 kg of CH_4 from the gasifier and 4.6 kg of gaseous hydrocarbons (with 4 or fewer carbon atoms) were combusted to create 0.1 kWh of electricity per Mg of MSW and 46 kg of CO_2. Like the gasifier emissions, only 19% of this CO_2 will contribute to GWP because the remaining 81% is biogenic in origin. The remaining 350 kg of hydrocarbons produced per megagram RDF gasified is syncrude. LCI data for petroleum refining is given in Table 6. Note that for every 1 kg of syncrude entering the refinery, only 0.98 kg of refined products is created due to losses in the refining process. After the syncrude yield was scaled to include mass loss, it was used to generate the refined product yields in Table 6. A complete system mass flow summary is presented in Appendix A.

Table 6 FT Products. The estimated syncrude yield is combined with refined product yield data to predict FT products.

FT Product	Yield (kg product produced/ kg syncrude) (NREL, 2012)	Mass (kg produced/ Mg MSW)	Volume (L produced / Mg MSW
Diesel	0.22	43	51
Gasoline	0.41	82	110
Liquefied Petroleum Gas (LPG)	0.026	5	10
Kerosene	0.089	18	23
Residual Fuel Oil	0.048	10	11
Refinery Gas	0.044	9	
Bitumen	0.036	7	
Petroleum Coke	0.058	12	
Petroleum Refining Coproduct	0.050	10	
Total	0.98	194	

3.4 Energy Consumption and Production

Energy consumption associated with material processing within the specified system boundary comes from electricity to power equipment and facilities, or fuel for transportation vehicles and rolling stock within the RDF facility. The system consumes 4.6 GJ of energy per Mg of MSW input and RDF with an energy content of 16.6 GJ/Mg. However, the energy content of the produced electricity and fuels for each Mg of MSW input is 9.7 GJ. Thus, the modeled system produces over 2.1 times as much energy as it consumes to convert the MSW feedstock into refined products. As shown in Figure 3, the gasification/FT facility consumes the most energy because of post-gasification syngas compression and the house load, which consume 68 % and 13% of total process-related energy consumption, respectively. However, the gasification/FT facility is also produces180kWh of electricity from heat recovery.

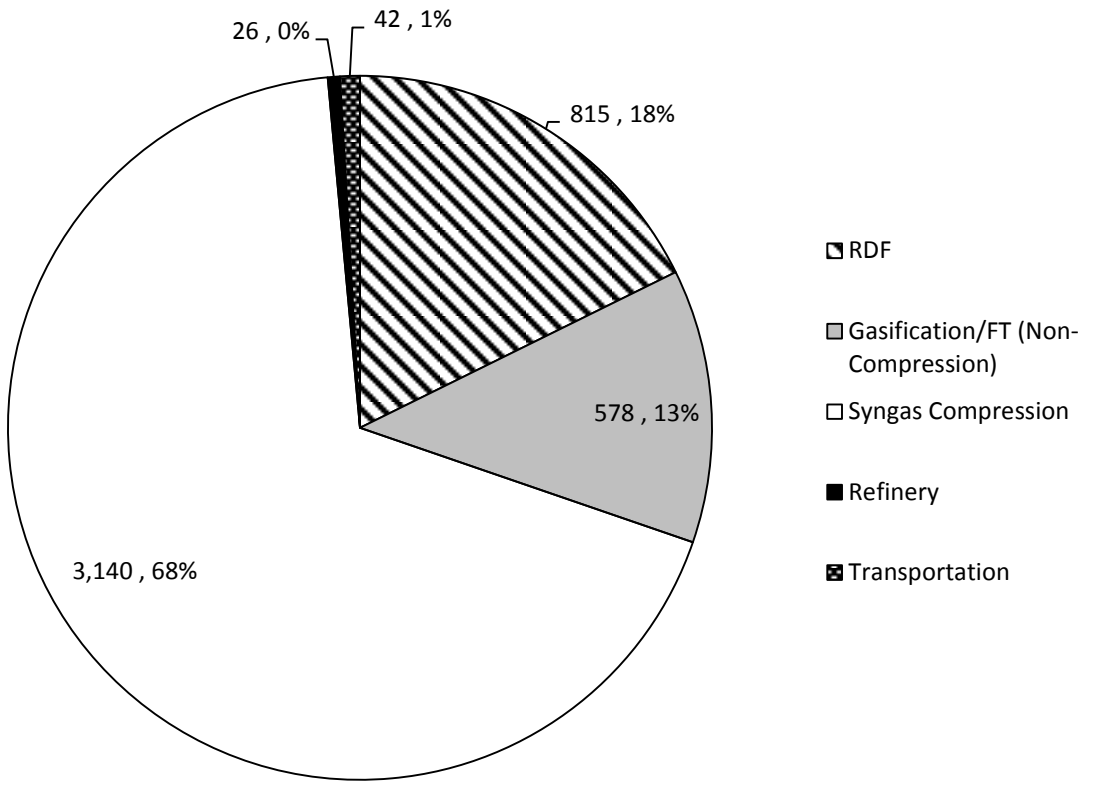

Figure 3 Energy consumption by process within the system boundary. The first number label represents the energy consumption per unit mass (MJ / Mg RDF) followed by the share of energy within the system boundary. Note that syngas compression required to achieve high FT conversion efficiencies requires the largest share of energy.

3.5 Process GWP

Emissions contributing to GWP result from process-related fuel and electricity consumption, gasification/FT emissions, and FT fuel combustion. The net GWP of this system is -112 kg CO_2-e per Mg MSW. This indicates that conventional petroleum conversion with identical products to the FT system combined with grid electricity of 180 kWh, has a higher GWP than the FT system, as shown in Figure 4. The emissions from

energy consumption and gasification/FT processes have a higher GWP than the offset pre-combustion emissions, which occur during the production of conventional petroleum derived fuels and products. However, FT fuel combustion has lower GWP than conventional fuels. Though both conventional petroleum derived fuels and MSW derived fuels have identical combustion emissions, the biogenic CO_2 does not contribute to GWP because it is created from the combustion of fuels derived from the biogenic components of RDF. Thus, combustion emissions from a fuel with only biogenic carbon would have no GWP, whereas combustion of a fuel made from only fossil carbon would have the same GWP as combustion of a conventional fossil fuel. Though 81% of RDF is biogenic, the combustion emissions from FT fuels are only 62% less than conventional fuels, as shown in Figure 4, because plastics generate more syngas and thus more fuel than biogenic components.

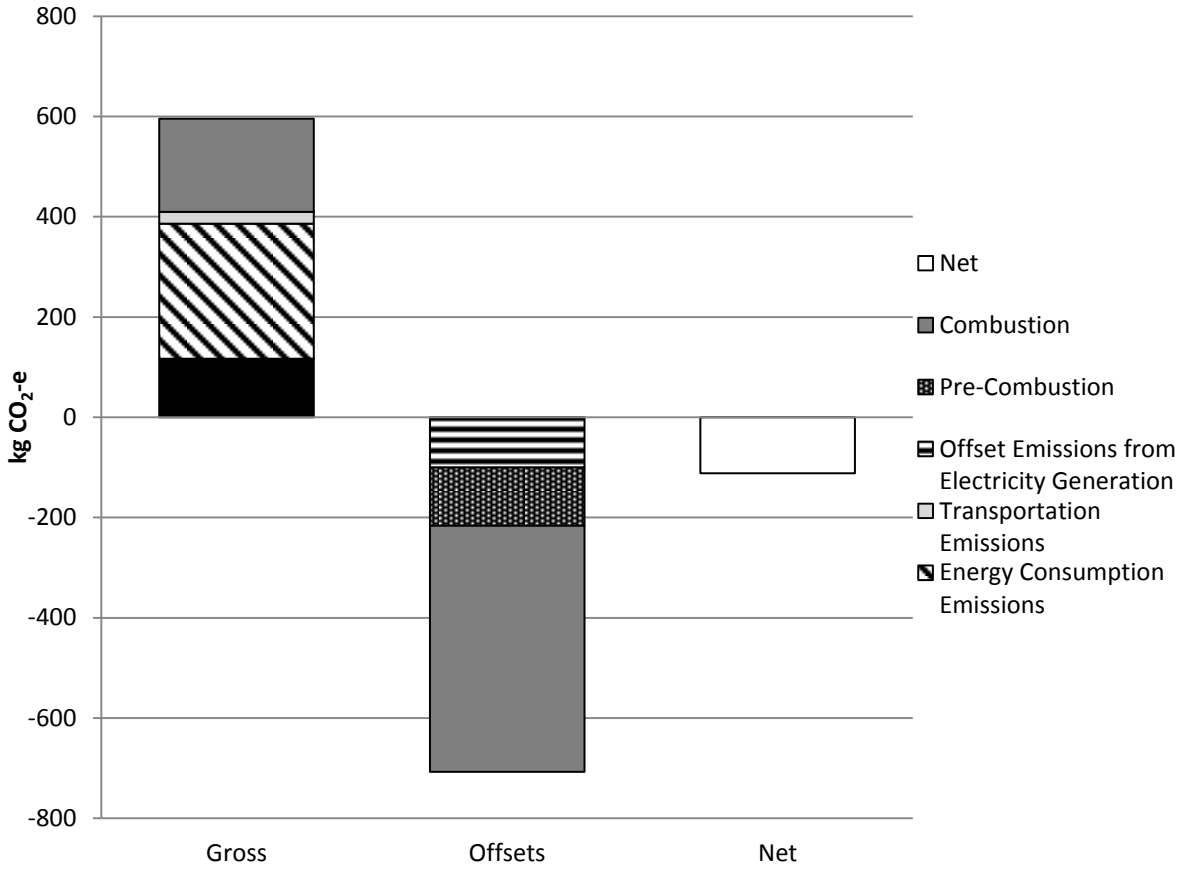

Figure 4 GWP for the MSW conversion process and the offsets associated with conventional petroleum processing. The net GWP represent the difference between gross emissions and the offsets.

3.6 Sensitivity Analysis

Model response to variations in input values was also explored. We performed a bounding analysis on waste composition by exploring changes to fiber and plastics content. The percentage of fiber and plastic were increased and decreased by 20% separately to create four new waste compositions. As each specified waste component was adjusted, the other waste components were scaled proportionally such that mass was conserved. For example, adjusting fiber content proportionally reduces the plastic and organics content.

When fiber content, composed of biogenic carbon, is increased or plastic content is decreased, the net GWP decreases. Because fiber has a lower syngas yield than plastic, waste compositions with higher fiber content produce less refined products than compositions with high plastic content, as shown by the magnitude of the offset bars in Figure 5. However, the high fiber compositions' lower gas volume requires less air compression energy, and fiber is removed early in the RDF process, as shown in Figure B1, which further reduces the energy requirement to make fuels from fiber. Figure 5 reveals that even as gross emissions deviate from the original composition up to 12%, the difference in net GWP between the default composition and each waste composition is within 9% of the initial gross emissions.

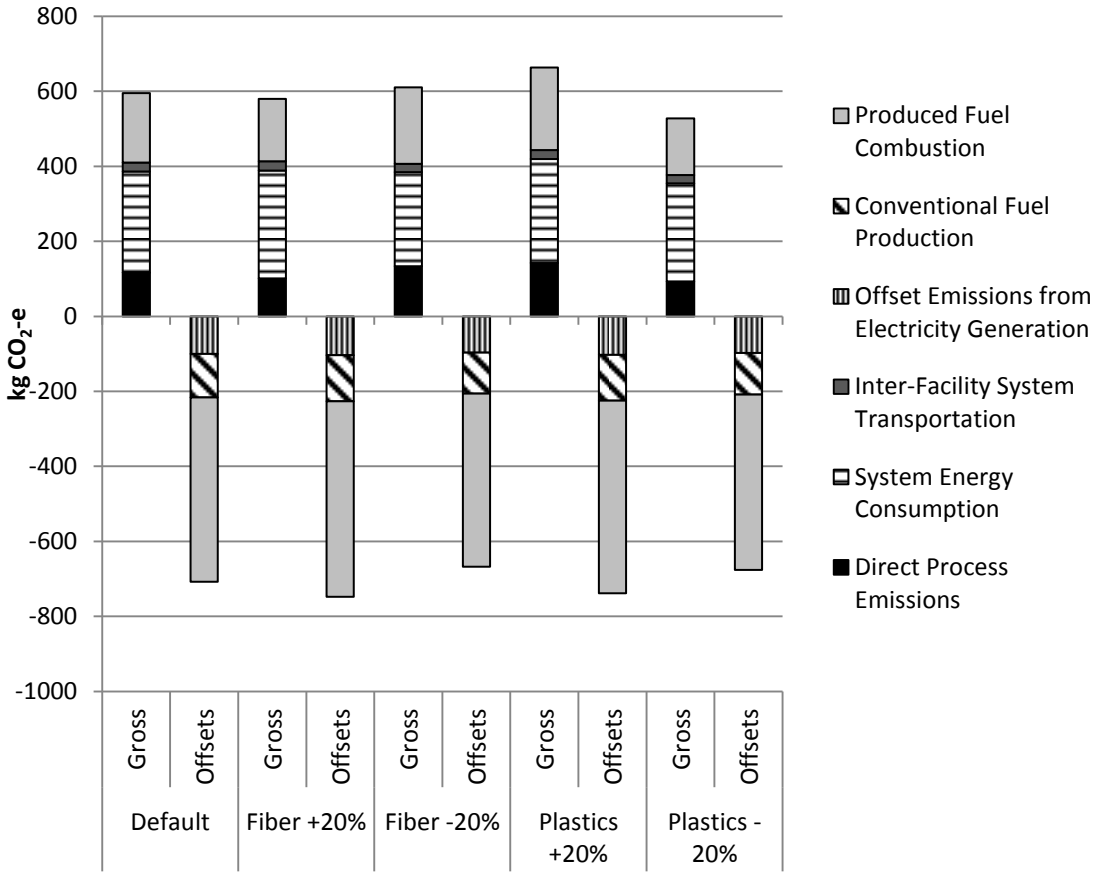

Figure 5 GWP of multiple waste compositions. Variations in fiber and plastic content alter both the gross system and offset GWP.

FT fuel yields vary less than 20% between waste compositions, as shown in Table 7. Net GWP changes between waste compositions, ranging between -57 and -149 kg CO_2-equivalents. However, these values are within 9% and 29%, as shown by the normalized net GWP in Table 7, of the corresponding gross GWP value, revealing both the offset and gross emissions are much larger than the net for all compositions. Because FT product yield varies little between waste compositions, the net GWP divided by the total FT product mass follows trends similar to the net GWP.

Table 7 GWP and Syncrude Yield for Multiple Waste Compositions. Varying waste composition changes GWP and syncrude yield.

Waste Composition	Net GWP (kg CO_2-e)	Total FT Product Mass (kg)	Net GWP/Mass FT Product (kg CO_2-e/kg product)	Normalized Net GWP (fraction of Gross GWP)
Default	-112	190	-0.59	-0.19
Fiber +20%	-168	210	-0.80	-0.29
Fiber -20%	-57	180	-0.31	-0.09
Plastics +20%	-76	200	-0.38	-0.11
Plastics -20%	-149	190	-0.78	-0.28

As the fiber fraction of RDF increases, the net GWP decreases while FT fuel production increases, due to an increased percentage of MSW going to RDF. The influence of fossil combustion emissions was also evident when the fossil fraction increased, through an increase in plastic content or a decrease in fiber content. GWP and fuel yield increased when plastic content increased. GWP also increased when fiber content decreased, indicating the decrease in the biogenic fraction of combustion emissions caused the GWP increase.

Changes to input parameters can alter environmental impacts directly, by effecting energy consumption and direct emissions, or indirectly, by effecting FT yield and the resulting offsets. To analyze how input parameters can directly affect environmental impacts, we explored model sensitivity to the compressor electricity requirement and the gasification and carbon intensity of grid electricity. The compressor electricity requirement was varied over a range from 50% less to 50% greater than the default value. The carbon intensity of grid electricity was varied from 0.28 to 0.67 kg CO_2-e/kWh. The lower bound represents implementation of a CO_2 policy requiring a 50% decrease in emissions, and the upper bound represents the average carbon intensity of electricity over the last half century based on US

EIA (2012), respectively. The GWP resulting from parameter variation, illustrated graphically in Figure 6, revealed that the air compressor electricity requirement changed the GWP linearly from -190 kg CO_2-equivalents at 50% of the initial value to -34 kg CO_2-equivalents at 150% of the initial value, which is a much larger than the range of -90 to -165 kg CO_2-equivalents created by the carbon intensity of grid electricity. If carbon intensity decreases, changes to the compressor electricity requirement will cause smaller variations in net GWP.

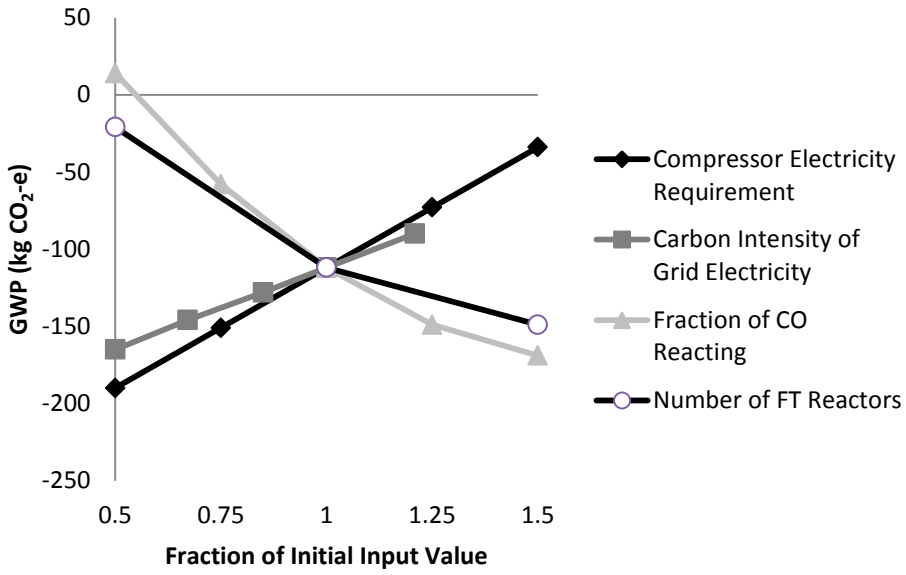

Figure 6 Model sensitivity to select parameters. As electricity demand increases and CO reacting decreases, GWP increases.

To explore the effect of modifying fuel yield on GWP, we separately varied the fraction of CO reacting in each reactor and the number of reactors from 50% to 150% of the initial values of 0.6 and 2, respectively. Both parameters display a negative exponential

relationship with net GWP. Because neither parameter is associated with energy consumption, the GWP effects are directly related to the fuel yield. The fraction of CO reacting had a GWP range of -169 to 14 kg of CO_2-equivalents, larger than the range from varying the number of reactors. However, the benefit to adding reactors should not be overlooked since it is simpler to add a reactor than reconfigure the entire system to get a higher CO reaction rate.

4. Discussion

The treatment of MSW via gasification and FT to create liquid fuels comparable to conventional refined petroleum products results in a GWP similar to conventional petroleum processing. Of course, this analysis did not address the finite nature of conventional fossil fuels and the need for alternative fuel sources. The produced electricity and FT fuels have cumulative energy content 2.1 times greater than the production system's energy requirement, making the system a net energy producer. A large share of the energy consumption associated with MSW conversion to liquid fuels is related to the compressor requirement for FT. Sensitivity analysis indicates that lower compression requirements combined with higher CO yields can produce liquid fuels with a GWP lower than conventional petroleum.

In addition, the model results indicate that changing MSW composition alters the magnitude of the net GWP. Plastics and fiber are the predominant RDF components, so variation in each was explored. Plastics were found to have higher syngas yields, in both the ASPEN Plus and spreadsheet models, which led to higher FT fuel yields than fiber. However, plastics have a higher combustion GWP due to their origin as conventional

petroleum. Thus, altering MSW composition allowed examination of the relative influence of increased yield and increased combustion GWP, as shown in Figure 5. Further analysis is required to quantify the effects of specific MSW policies on GWP, but model results suggest that removing plastics from MSW, via a recycling policy, would increase the environmental benefits of FT fuels at the expense of fuel yield.

Parametric sensitivity analysis of the air compression energy requirement, carbon intensity of electricity, CO reacting percentage, and number of FT reactors was used to quantify their effects on GWP. Because syngas compression accounts for 68% of the total energy consumption, we explored the effect of altering the compression electricity requirement. If more compression is required to get the partial pressures of CO and H_2 into acceptable ranges, the energy requirement will increase. However, the energy requirement could decrease if advancement in FT technology allowed for partial pressure requirements to decrease without affecting product yield. In the case where the compression energy requirement decreased 50%, the system energy consumption decreased to 3030 MJ/Mg, a 34% reduction in total system energy. An alternative approach is to operate the gasifier under pressurized and/or oxygen feed conditions. The limitation of the scale of MSW gasifiers, however, may not justify the use of such gasification systems from a capital expense standpoint.

FT yield is most affected by the fraction of CO reacting and the number of FT reactors in series in the model, for a given α-value. The fraction of CO reacting affected yield more than the number of FT reactors, as shown in Figure 6. However, if the fraction of CO reacting is low, the number of reactors becomes more important. Once a FT system is fully-

operational, adjusting the number of reactors may be more practical than altering the components of the FT system to increase FT fuel yield.

The gasification and FT system's GWP may be affected by changes to the national energy system. If the carbon intensity associated with grid electricity decreases, the energy consumption GWP will decrease, increasing the environmental benefits of this fuel-producing system, as shown in Figure 6. Similarly, if the market share of biofuels increases, the GWP associated with the MSW-derived fuel will increase because combustion emission offsets will be less. On the other hand, it is possible that a move towards liquid transportation fuels derived from oil shale or oil sands with significantly higher GWP would result in a proportional reduction in the GWP of MSW-derived fuel. Such exogenous factors can affect the overall environmental performance of the system, and further analysis is needed to determine how changes to the broader energy system would affect the GWP of the studied system.

The results in this paper reflect only a portion of an MSW system. Prior to comparison with other MSW treatment methods, care must be taken to ensure system equivalence. For example, residuals from both the RDF facility and gasifier must be treated using modeling assumptions consistent with the MSW treatment schemes. Use of other LCA process models is required to construct systems comparable with other MSW treatment schemes.

REFERENCES

Ahmed, I., Gupta, A.K., 2009. Evolution of syngas from cardboard gasification. Applied Energy 86, 1732–1740.

Ahmed, I.I., Nipattummakul, N., Gupta, A.K., 2011. Characteristics of syngas from co-gasification of polyethylene and woodchips. Applied Energy 88, 165–174.

Ammendola, P., Chirone, R., Miccio, F., Ruoppolo, G., Scala, F., 2011. Devolatilization and Attrition Behavior of Fuel Pellets during Fluidized-Bed Gasification. Energy Fuels 25, 1260–1266.

Belgiorno, V., De Feo, G., Della Rocca, C., Napoli, R.M.A., 2003. Energy from gasification of solid wastes. Waste Management 23, 1–15.

Cao, Y., Gao, Z., Jin, J., Zhou, H., Cohron, M., Zhao, H., Liu, H., Pan, W., 2008. Synthesis Gas Production with an Adjustable H2/CO Ratio through the Coal Gasification Process: Effects of Coal Ranks And Methane Addition. Energy Fuels 22, 1720–1730.

Claeys, M., van Steen, E., 2004. Basic Studies, in: Fischer-Tropsch Technology, Studies in Surface Science and Catalysis. Elsevier B.V.

Combs, A., 2012. Life Cycle Analysis of Recycling Facilities in a Carbon Constrained World.

Ecoinvent Data V2.2, 2010.

Energy Centre of the Netherlands, 2012. Phyllis2.

Flory, P.J., 1936. Molecular Size Distribution in Linear Condensation Polymers1. J. Am. Chem. Soc. 58, 1877–1885.

Fock, F., Thomsen, K.P.B., Houbak, N., Henrikson, U., 2000. Modelling a biomass gasification system by means of "EES", in: Scandinavian Simulation Society. Presented at the SIMS 2000 Conference, Kgs. Lyngby, Denmark.

Gai, C., Dong, Y., 2012. Experimental study on non-woody biomass gasification in a downdraft gasifier. International Journal of Hydrogen Energy 37, 4935–4944.

Harrison, K.W., Dumas, R.D., Barlaz, M.A., Nishtala, S.R., 2000. A Life-Cycle Inventory Model of Municipal Solid Waste Combustion. Journal of the Air & Waste Management Association 50, 993–1003.

Kaplan, P.O., DeCarolis, J., Thorneloe, S., 2009. Is It Better To Burn or Bury Waste for Clean Electricity Generation? Environ. Sci. Technol. 43, 1711–1717.

Koehler, A., Peyer, F., Salzmann, C., Saner, D., 2011. Probabilistic and Technology-Specific Modeling of Emissions from Municipal Solid-Waste Incineration. Environ. Sci. Technol. 45, 3487–3495.

Levis, J.W., Barlaz, M.A., 2011. Is Biodegradability a Desirable Attribute for Discarded Solid Waste? Perspectives from a National Landfill Greenhouse Gas Inventory Model. Environ. Sci. Technol. 45, 5470–5476.

Marano, J.J., Ciferno, J.P., 2001. Life-Cycle Greenhouse-Gas Emissions Inventory For Fischer-Tropsch Fuels.

Ménard, J.-F., Lesage, P., Deschênes, L., Samson, R., 2004. Comparative life cycle assessment of two landfill technologies for the treatment of municipal solid waste. Int J LCA 9, 371–378.

National Renewable Energy Laboratory, 2012. U.S. Life-Cycle Inventory Database V1.1.

Pellegrino, J., Brueske, S., Carole, T., Andres, H., 2007. Energy and Environmental Profile of the U.S. Petroleum Refining Industry.

Pytlar, T.S., 2010. Status of Existing Biomass Gasification and Pyrolysis Facilities in North America. Presented at the 18th Annual North American Waste-to-Energy Conference.

Riber, C., Bhander, G.S., Christensen, T.H., 2008. Environmental assessment of waste incineration in a life-cycle-perspective (EASEWASTE). Waste Manag Res 26, 96–103.

RTI International, 2012. Environmental and Economic Analysis of Emerging Plastics Conversion Technologies.

Ruoppolo, G., Ammendola, P., Chirone, R., Miccio, F., 2012. H2-rich syngas production by fluidized bed gasification of biomass and plastic fuel. Waste Management 32, 724–732.

Spath, P.L., Dayton, D.C., 2003. Preliminary Screening — Technical and Economic Assessment of Synthesis Gas to Fuels and Chemicals with Emphasis on the Potential for Biomass-Derived Syngas.

Swain, P.K., Das, L.M., Naik, S.N., 2011. Biomass to liquid: A prospective challenge to research and development in 21st century. Renewable and Sustainable Energy Reviews 15, 4917–4933.

United States Energy Information Administration, 2012. Annual Energy Review.

United States Environmental Protection Agency, 2010. Municipal Solid Waste Generation, Recycling, and Disposal in the United States: Facts and Figures for 2010.

Vera, D., de Mena, B., Jurado, F., Schories, G., 2013. Study of a downdraft gasifier and gas engine fueled with olive oil industry wastes. Applied Thermal Engineering 51, 119–129.

APPENDICES

Appendix A. Input Data

Table A1 Inter-facility transport distance in km. Calculated impacts include transport between system facilities, which depend on the travel distances for each mode of transportation. All non-refinery distances reflect local truck transport. Gasifier/FT to Refinery distances indicate transport from Raleigh, NC to Galvaston, TX, a scenario representative of east coast transport.

From	To	Heavy-duty Truck	Ocean Freighter
RDF Facility	Landfill	25	
RDF Facility	Gasifier/F-T	25	
Gasifier/F-T	Ash Landfill	25	
Gasifier/F-T	Refinery	250	2700

Table A2 As Generated Waste Composition based on USEPA (2010).

Waste Categories	Waste Component	Contribution to As-Generated MSW (%)
Yard Waste[a]	Leaves	7%
	Grass	5%
Food Waste[b]	Vegetable	15%
	Non-Vegetable	4%
Recyclable Paper	Newsprint	5%
	Corrugated Cardboard	15%
	Office Paper	3%
	Magazines	1%
	3rd Class Mail	2%
Recyclable Plastic	HDPE Containers	1%
	PET Containers	1%
	Plastic Film	2%
Recyclable Metals	Ferrous Cans	1%
	Aluminum Cans	1%
Glass	Brown	3%
	Green	1%
	Clear	1%
Non-Recyclable	Paper	11%
	Plastic	6%
Other	Rubber/Leather	1%
	Wood	5%
	Textiles	5%
	Miscellaneous Inorganic	4%

[a] The leaves and grass proportions are based on Staley et al. (2009)
[b] Vegetable waste is assumed to be 80% of food waste.

Appendix B. RDF Model

Municipal solid waste (MSW) must be processed prior to treatment by gasification. This processing stage separates materials with high calorific values from materials with lower calorific value. The high calorific materials are pelletized into refuse derived fuel (RDF), while aluminum and ferrous materials are separated for recycling. The residual may be treated via landfill, composting or anaerobic digestion. The RDF process model calculates energy use and environmental impacts associated with the process of transforming waste, as collected, into a fuel, either loose or pelletized, for use in a gasifier.

Process Flow

As shown in Figure 1, the MSW first enters a flail mill to open bags and reduce waste size. The waste proceeds to a trommel that removes waste smaller than two inches. The trommel “unders”, which consist primarily of food waste, yard waste, and broken glass, are passed under a magnet to remove ferrous metal for recycling. The trommel unders can be landfilled directly or treated biologically by composting or anaerobic digestion.

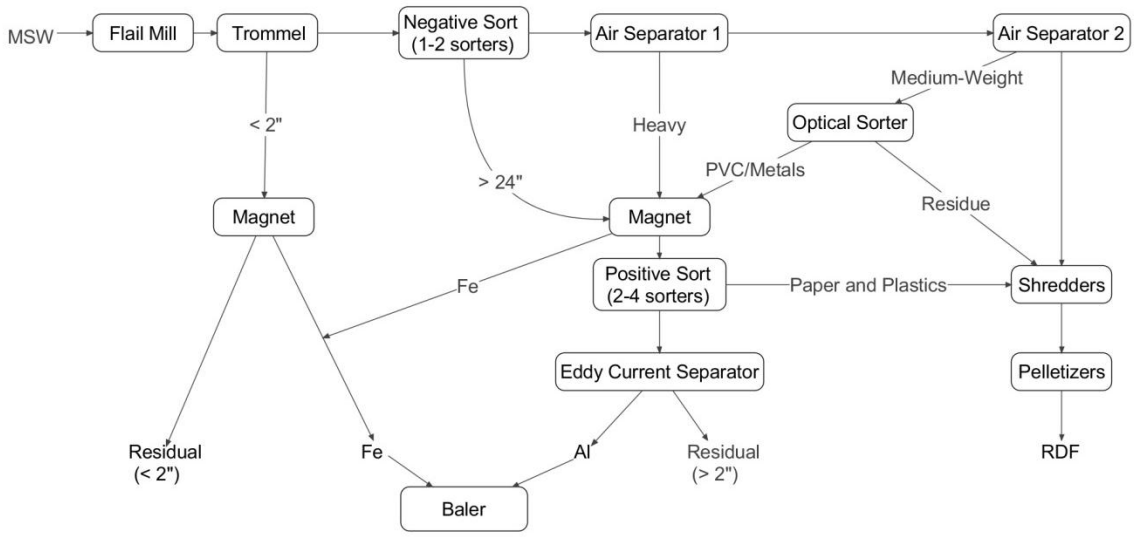

Figure B1 RDF Process Flow Diagram. During the production of RDF, materials undesirable for gasification are removed via mechanical sorting.

Waste stream components greater than 2 inches proceed from the trommel to a negative manual sort. Pickers remove materials larger than 24 inches and send them to a residual stream.

The waste stream containing materials between 2 and 24 inches goes through 2 air separators. The first air separator separates the heavy material (e.g., metals, glass, wet materials) from the light weight (e.g., paper, plastic) material. The heavy material goes to a residual stream. The light weight material goes through another air separator that separates light material from medium-weight material. The medium weight material goes to an optical sorter that ejects PVC and metals into a residual stream and sends all other medium weight material to a shredder.

The ejected PVC and metals are mixed into a residual stream with the manually sorted non-combustible materials larger than 24 inches and the heavy materials. This residual stream is passed under a magnet to remove ferrous materials. The remaining stream passes through a positive manual sort, where pickers remove high calorific materials from the residual stream. All other materials pass through an eddy current separator to remove aluminum. The residual from the eddy current separator will most likely be landfilled. This residual stream contains materials that are neither recyclable nor beneficial to gasify. Some materials, like PVC, have the potential to increase harmful emissions (Velis et. al 2011). A shredder reduces the size of the light materials, optical sorter residual, and manually selected materials. The shredded material is then pelletized into RDF.

Model Functionality

The user can specify whether each piece of equipment is present, in part pelletization is not strictly necessary. When the user specifies the equipment as not present, resource consumption is not allocated to any mass, which prevents the non-present equipment from contributing to total energy consumption. To accurately reflect mass flow, no mass will be removed when equipment is not present. The total equipment throughput, which is used to calculate conveyor electricity use, is also set to zero when equipment is not present to prevent unnecessary conveyors from being included in energy consumption. All equipment can be indicated as not present in the system, but the effect of removing equipment other than the pelletizers on the final RDF composition and the overall system should be carefully examined prior to analysis.

Users can input a waste composition and equipment data (e.g., separation efficiencies, throughput, motor size) or use default values. Each piece of equipment has a column in a separation efficiency matrix that contains a row for each waste fraction (Table 1). Displaying separation efficiencies in a matrix allows efficiencies to vary across waste fractions for a single piece of equipment. Though different efficiencies are not necessary for every piece of equipment, variation in size and material properties within a single waste fraction creates the need for multiple efficiencies. Though the default efficiency values do not account for unintended material removal (e.g. a magnet removing paper attached to ferrous material), the separation matrix has the ability to track impurities in the waste streams.

Table B1 Sample Separation Efficiency Matrix

Waste Categories	Waste Component	Trommel	Air Separator
Yard Waste	Leaves	70%	
	Grass	70%	90%
Food Waste	Vegetable	70%	90%
	Non-Vegetable	70%	90%
Recyclable Paper	Newsprint		
	Corrugated Cardboard		
	Office Paper		
	Magazines		
	3rd Class Mail		
Recyclable Plastic	HDPE Containers		
	PET Containers		
	Plastic Film		
Recyclable Metals	Ferrous Cans		90%
	Aluminum Cans		90%
Glass	Brown		100%
	Green		100%
	Clear		100%
Non-Recyclable	Paper		
	Plastic		
Other	Rubber/Leather		90%
	Wood		90%
	Textiles		
	Miscellaneous Inorganic		100%

Mass Flow

The functional unit for the modeled system is 1 Mg of MSW delivered to the RDF pland upstream of the gasifier. Though this model initially calculates the emissions associated with 1 Mg of each waste fraction, emissions are later scaled to reflect the user's input waste composition. The initial input vector is multiplied by the separation efficiency matrix to calculate the mass removed (Equation B1).

$$M_{\mathrm{Re}moved,i,j} = M_{Input,i,j} \bullet S_{i,j} \quad \text{(B1)}$$

$M_{removed,i,j}$: The mass of waste fraction *i* removed by equipment *j*
$M_{Input,i,j}$: The mass of waste fraction *i* entering equipment *j*
$S_{i,j}$: The fraction of waste fraction *i* removed with equipment *j*

The mass remaining in the waste stream, referred to as the mass exiting the equipment, is calculated by subtracting the removed mass from the input mass (Equation B2).

$$M_{Exiting,i,j} = M_{Input,i,j} - M_{\mathrm{Re}moved,i,j} \quad \text{(B2)}$$

$M_{Exiting,i,j}$: The mass of waste fraction *i* remaining in the waste stream after passing through equipment *j*.

The mass flow throughout the system is calculated using Equations B1 and B2. The inputs to each piece of equipment are calculated as mass removed or mass exiting previous equipment, with values summed where applicable.

Energy Consumption in the RDF Plant

Data for individual equipment is used to find the total energy consumption per waste fraction. For each piece of equipment, the rated motor size is multiplied by a motor capacity factor, which is then divided by the equipment throughput and a throughput capacity factor (Equation 3, based on Combs, 2012).

$$E_{eq,j} = \frac{E_{motor,j} \bullet C_{motor,j}}{M_{throughput,j} \bullet C_{throughput,j}} \quad \text{(B3)}$$

$E_{eq,j}$: Electricity consumption in kilowatt-hours per megagram for equipment *j*.
$E_{motor,j}$: Rated motor size in kilowatts.
$C_{motor,j}$: Motor capacity factor
$M_{throughput,j}$: Throughput of equipment *j* in megagrams per hour
$C_{throughput,j}$: Throughput capacity factor

The motor capacity factor accounts for a motor not utilizing all possible power. From vendor discussions, motor electricity use ranges between one third and one half of the rated motor size. The throughput capacity factor adjusts for equipment operating with less than maximum throughput. These capacity factors allow the model to better reflect the energy associated with each waste fraction. The equipment electricity usages calculated with Equation B3 are shown in Table B2.

Table B2 Equipment Electricity Usage per Mg of Throughput

Equipment	**Electricity Consumption (kWh/Mg)**	**Diesel Consumption (L/Mg)**
Conveyor	0.1	0
Flail Mill	4.0	0
Trommel 2"	0.8	0
Negative Sort (> 24")	0.9	0
Air Separator 1	2.7	0
Air Separator 2	2.7	0
Magnet 1	1.2	0
Optical Sorter	4.7	0
Magnet 2	1.2	0
Positive Sort	0.9	0
Eddy Current Separator	0.4	0
Shredders	17.6	0
Pelletizers	26.1	0
Baler	1.0	0
Rolling Stock	0.0	10

Total electricity consumption for each waste fraction is calculated by summing the electricity associated with equipment, offices, and the factory floor (Equation B4).

$$E_{total,i} = \sum_j M_{us,i,j} \bullet E_{eq,j} + \sum_j M_{tp,i,j} \bullet E_{con} + E_{office} + E_{floor} \quad \text{(B4)}$$

$E_{total,i}$: Total electricity consumption of processing one megagram of waste fraction *i*
$M_{us,i,j}$: User specified mass used for resource allocation, which could be the total throughput of equipment *j*, mass removed by equipment *j*, or mass remaining in the waste stream after equipment *j*.
$M_{tp,i,j}$: Total mass throughput of waste fraction *i* through equipment *j*.
E_{con}: Conveyors' electricity consumption per megagram
E_{office}: Electricity consumption per megagram in on-site offices
E_{floor}: Non-equipment electricity consumption on the warehouse floor.

The equipment electricity usage per waste fraction is calculated in the spreadsheet model by summing the product of a row in its "Mass Used for Resource Calculation" matrix by the column of electricity consumption per megagram in its "Equipment" table. The masses used in this calculation are a combination of total equipment throughput, mass removed, and mass remaining in waste stream. The differentiation is needed because some equipment targets removal of material undesirable for gasification (e.g. magnet, eddy current separator), while other equipment removes materials desirable from the waste stream (e.g. air separators). Conveyors and flail mills do not remove any mass, so the total throughput option is needed for resource calculations. Default masses have been selected, but the user has the option to change the selected mass. This feature is intended to allow flexibility in the model if data for a different type of equipment were input. Because the energy consumption values are recalculated to reflect any change in mass type, users must carefully examine the change in values to assure the final consumption values reflect the intended system.

Unlike other equipment in an RDF facility, multiple conveyors are present to transport waste to each piece of equipment. The total energy consumption associated with conveyors is calculated in a unique manner. The energy consumption per megagram is

multiplied by a sum of the initial input and total equipment throughputs for all present equipment except the baler and rolling stock. This approach assumes all conveyors contain equally sized motors and the electricity consumed by each conveyor is linear with respect to throughput. Because of this linear assumption, the number of conveyors present in the system is not needed to calculate electricity use. Thus, two conveyors carrying 0.5 Mg per hour use the same electricity as a single conveyor carrying 1.0 Mg per hour.

Since electricity consumption is calculated per Mg and the total electricity consumption is aggregated per Mg, the office and floor electricity consumption values can be added directly to the equipment electricity consumption. The office electricity use is calculated by multiplying daily office electricity consumption per square meter, based on data from CBECS 2003, by industry data for floor area per throughput and the fraction of total facility area attributed to offices (Equation B5).

$$E_{office} = e_{office} \bullet R_{fa} \bullet f_{office} \quad \text{(B5)}$$

e_{office}: daily office electricity use per square meter
R_{fa}: Floor area in square meters per megagram of daily facility throughput
f_{office}: Fraction of floor area occupied by offices

Similarly, electricity consumption on the warehouse floor is calculated by multiplying daily warehouse floor electricity consumption per square meter, from CBECS 2003, by the same floor area per throughput used to calculate office electricity consumption and the fraction of office floor area subtracted from one (Equation B6).

$$E_{floor} = e_{floor} \bullet R_{fa} \bullet (1 - f_{office}) \quad \text{(B6)}$$

e_{floor}: daily warehouse electricity use per square meter

All diesel and propane consumption occurs in waste processing equipment (Equation B7 & B8). The default values only have a diesel consumption value for rolling stock and do not include any propane consumption.

$$D_{total,i} = \sum_j M_{us,i,j} \bullet D_j \quad \text{(B7)}$$

$D_{total,i}$: Total diesel consumed treating one megagram of waste fraction *i*.
D_j: Diesel consumption per megagram of equipment *j*

$$P_{total,i} = \sum_j M_{us,i,j} \bullet P_j \quad \text{(B8)}$$

$P_{total,i}$: Total propane consumed treating one megagram of waste fraction *i*
P_j: Propane consumption per megagram of equipment *j*

Emissions

Total air and water emissions associated with RDF manufacture are calculated by aggregating emissions associated with resource consumption (Equation B9).

$$N_{k,i} = E_{total,i} \bullet R_{E,k} + D_{total,i} \bullet R_{D,k} + \mathrm{P}_{total,i} \bullet R_{P,k} \quad \text{(B9)}$$

$N_{k,i}$: Emission *k* per unit mass attributed to waste fraction *i*
$R_{E,k}$: Rate of emission *k* resulting from electricity production, distribution, and consumption
$R_{D,k}$: Rate of emission *k* resulting from diesel production, distribution, and consumption
$R_{P,k}$: Rate of emission *k* resulting from propane production, distribution, and consumption

The initial emissions values correspond to one megagram of each waste fraction. The emissions associated with the input waste composition multiply these initial calculated emission values by each waste component's contribution to the waste composition (Equation B10).

$$U_{k,i} = N_{k,i} \bullet f_i \qquad \text{(B10)}$$

$U_{k,i}$: Mass of emissions k attributed to waste fraction i based on user input waste composition.

f_i: Fraction that waste fraction i contributes to overall composition

Appendix C. Gasification Model Equations and Comparison with ASPEN Plus

The spreadsheet gasification model estimates syngas yield and composition using a mass balance approach with feedstock material properties and gasifier performance parameters. The system mass balance equation, shown in equation 1, is modeled as elemental mass balances for carbon, hydrogen, and oxygen. When these equations are combined with the H_2 to CO ratio, CH_4 production rate, and ash content, yields for individual syngas components (i.e., CO, H_2, CO_2) can be estimated. The carbon, hydrogen, and oxygen balances are shown in equations C1, C2, and C3 respectively.

$$C_i = C_{CO,i} + C_{CH_4,i} + C_{ash,i} + C_{CO_2,i} \text{ (Equation C1)}$$

where:
C_i=mass of carbon bound in m_i
$C_{CO,i}$=mass of carbon bound in $m_{CO,i}$
$C_{CH4,i}$=mass of carbon bound in $m_{CH4,i}$
$C_{ash,i}$=mass of carbon bound in $m_{aah,i}$
$C_{CO2,i}$=mass of carbon bound in $m_{CO2,i}$

$$H_i + 2 \bullet H_{s,i} = 4 \bullet H_{CH_4,i} + 2 \bullet H_{H_2O,i} + 2 \bullet H_{H_2,i} \text{ (Equation C2)}$$

where:
H_i=mass of hydrogen bound in m_i
$H_{S,i}$=mass of hydrogen bound in $m_{S,i}$
$H_{CH4,i}$=mass of hydrogen bound in $m_{CH4,i}$
$H_{H2O,i}$=mass of hydrogen bound in m_{H2O}
$H_{H2,i}$=mass of hydrogen bound in $m_{H2,i}$

$$O_i + O_{s,i} + 2 \bullet O_{air,i} = 2 \bullet O_{CO_2,i} + O_{H_2O,i} + O_{CO,i}$$ (Equation C3)

where:
O_i=mass of oxygen bound in m_i
$O_{S,i}$=mass of oxygen bound in $m_{S,i}$
$O_{air,i}$=mass of oxygen bound in $m_{air,i}$
$O_{CO2,i}$=mass of oxygen bound in $m_{CO2,i}$
$O_{H2O,i}$=mass of oxygen bound in m_{H2O}
$O_{CO,i}$=mass of oxygen bound in $m_{CO,i}$

ASPEN Plus and Spreadsheet Comparison

To validate the mass-balance spreadsheet model, the syngas yield was compared with the ASPEN Plus model used to generate the H_2 to CO and air to feedstock mass ratios. Results were compared for feedstocks representative of fiber, plastics, and organic materials found in MSW. Table C1 shows the syngas component yields for each feedstock, assuming 0% of the total solids is converted to CH_4. When data were available for the feedstock at multiple moisture contents (i.e., dry, as-received), both were input to the model to explore the spreadsheet model's response to variations in moisture content. The as-received moisture content values reflect feedstock moisture content without drying prior to ultimate analysis for determination of its chemical properties. The model predicted CO and H_2 yields for all feedstocks are within 10% of the ASPEN Plus results, except for the willow feedstock with 43.5% moisture content. However, the spreadsheet deviated low in all estimates of CO_2 production, which does not have a significant effect on downstream process yield estimates. Because direct emissions are only a small fraction of GWP in all scenarios, the low CO_2 estimates do not noticeably impact the GWP estimates.

Table C1 Difference between spreadsheet model and ASPEN Plus yield estimates with 0% CH_4

	Difference[3] (%)			Difference (10^3 moles/Mg feedstock)		
Feedstock	CO	H_2	CO_2	CO	H_2	CO_2
Corn Stover-Dry	3	3	-17	0.9	0.6	-10.7
As received (6.1% MC)	-7	-7	-11	-1.8	-1.4	-11.2
Paper, mixed paper, pellet dry	0	0	-16	-0.1	-0.1	-7.2
As received (7.2% MC)	-10	-10	-10	-2.3	-2.2	-7.9
HDPE	1	1	-100	0.4	0.4	-0.9
PET	5	5	-42	2.1	0.8	-6.3
Willow-Dry	6	6	-17	1.7	1.1	-13.0
As received (43.5% MC)	-73	-73	-20	-7.8	-11.6	-12.9
Switchgrass	3	3	-18	0.8	0.5	-12.4

Biomass gasification typically yields about 3% CH_4 by mass (Southern Research Institute, Personal Communication). In an effort to better model gasification, we specified 3% CH_4 for all biogenic feedstocks. ASPEN Plus simulations for all biogenic feedstocks, including additional willow feedstocks with varying moisture content, were conducted for comparison with the spreadsheet model at 3% CH_4, as shown in Table C2. In the case of willows, we found significant deviation (+50%) from model results for moisture contents as low as 10%. Further exploration of the effects of willow moisture content on model results is needed to determine bounds for fiber, plastic, and other waste components likely to be found in RDF. However, the spreadsheet model produces syngas yields within 20% of comparable ASPEN Plus simulations for all MSW components feedstocks used in this analysis.

[3] Percent difference was calculated by dividing the difference of the spreadsheet model result and the ASPEN Plus result by the ASPEN Plus result.

Table C2 Difference between spreadsheet model and ASPEN Plus yield estimates with 3% CH_4

	Difference (%)					**Difference (10^3 moles/Mg)**				
	CO	H_2	CH_4	CO_2	H_2O	CO	H_2	CH_4	CO_2	H_2O
Corn Stover-Dry	-7	-7	-1	5	10	-2.4	-1.5	-4.2	4.4	0.5
As received (6.1% MC)	-20	-20	-1	5	6	-4.7	-3.3	-10.3	10.9	0.6
Paper,mixed paper, pellet dry	-7	-7	-2	3	25	-2.1	-1.7	-0.9	0.9	0.7
As received (7.2% MC)	-16	-16	-1	2	15	-4.0	-3.7	-2.7	2.8	0.8
Willow-Dry	-6	-6	-1	3	3	-2.0	-1.2	-6.5	6.7	0.2
(10.9 % MC)	-52	-52	-1	56	43	-17.2	-13.1	-8.1	13.5	4.1
(21.78 % MC)	-63	-63	-1	35	38	-15.4	-14.6	-9.3	13.1	5.1
(32.6 % MC)	-70	-70	-1	6	29	-12.1	-14.2	-10.3	11.0	5.0
As received (43.5% MC)	-81	-81	-1	-15	23	-9.0	-13.2	-10.9	9.0	5.3
Switchgrass	-10	-10	-1	6	15	-3.0	-1.9	-6.0	6.4	0.9